THEORETICAL ANALYSIS OF SHEAR SLITTING OF PAPER ON THE BASIS OF A THREE-DIMENSIONAL MATERIAL LAW

by

E. G. Welp and E.Wolf

Ruhr-University Bochum
Germany

ABSTRACT

The slitting and cross cutting as one of the substantial manufacturing methods in paper equipment and paper processing, are characterized in many applications by practice problems, which lead to productivity and quality losses.

Analysing the knowledge of shear-slitting shows, that there are great gaps in the fundamental understanding of the slitting procedure as well as in its conversion to mechanical engineering. For this reason our institute carries out a research project to analyse the slitting procedure on a theoretical and experimental basis. The aim of this project is to clear up the correlations of shear-slitting and to derive measures for the improvement of slit quality and blade durability in practice.

Because of the complex, three-dimensional state of stress during the slitting process, the problem cannot be solved analytically and the finite-element-method is used to calculate the states of stress and strain. For the modelling of the material behavior of paper, a three-dimensional material law is deduced. The influence of the material law and the cutting tool geometry on the sher slitting process is studied. The achieved results of the FEM-analysis shall be compared to experimental results in later research work.

NOMENCLATURE

E	Young's modulus
C	Stiffness matrix
G	Shear Modulus
S	Tension border
ε	Strain
μ	Poisson's ratio

σ Stress

subscripts:
1 Machine direction - MD
2 Cross direction - CD
3 Thickness direction - ZD
I Principal stress
ini Initial value

INTRODUCTION

The mechanical slitting technique represents the most frequently procedure for the separation of products in the paper-processing industry. The industrial practice problems with shear-slitting of paper are frequently tried to be solved by trial-and-error procedures. Concrete proposals for solving or avoiding production problems within the range of slitting technique are not to be found [1], [2]. In order to be able to understand the elementary procedures of the conventional slitting technique, a purposeful analysis of all possible factors of influence e.g.: the slitting procedure, the material properties and the cutting tool is necessary. With an exact knowledge of these influence the correlations of shear-slitting can be cleared up and measures for practice for the improvement of productivity and blade durability can be derived.

THE SHEAR-SLITTING OF PAPER - STATE-OF-THE-ART

Shear-slitting is defined as dividing workpieces by means of the slitting surface of two tools, which move very close to each other. The separation of the workpiece results predominantly from the sliding between the workpiece and the cut material in the slitting area [3].

The first and the most extensive investigations of the slitting process are found in the area of slitting sheet metal processing. These works are mostly carried out experimentally and are dealing with slitting forces during the slitting process, the necessary slitting performance and the durability of cutting tools, e. g. [6], [7] and [9].

A more detailed investigation in shear-slitting process is done by Stromberger and Thomsen [5]. On the basis of microscopic investigations of the plane in the section of punched sheet metals they determined, that the slitting process takes place in three phases: the compression -, the slitting - and the tearing phase. The compression phase begins with the contact between the cutting tool and the sheet of paper. If pressure forces affect the blade, the paper is distorted and compressed underneath the cutting tool. As soon as a certain maximum shear stress, a result of the tension in MD and compression in CD, is reached, the separation of the material begins. The shear stress has exceeded the shear-yield-border. Due to the state of stress in the material a cracking begins directly at the

knife edge toward the maximum compressive stress. In case of increasing the outside load the next material-specific border is reached, the shear-break-border. This border marks the beginning of the tearing phase. The relation between normal stress, the resulting shear stress and the material specific stress-borders can be easily shown by use of Mohr´s circle, as shown in figure 1. In the last phase of the slitting process, the tearing phase, the wedge effect of the cutting tool plays a central role. The wedge-shaped geometry of the cutting tool causes an increased material displacement on the wedge surface side. Thus it comes to an uncontrolled destruction of the remainded part of the paper web.

A similar description of the cutting process comes from Siebel [8]. His work refers to the material behavior of the cut material during the slitting process. He investigates the borders of the three slitting phases and tries to separate them. In addition to this he connects the separation process with the parabolic material failure theory by Mohr-Coulomb and describes the material-specific failure borders.

The three-phase theory of the separation process was applicated on paper and cardboard by Hombach and Storm [4]. Following their statement it is sufficient to observe the plastic deformations of paper within the slitting process with the shear stress hypothesis.

The modelling of the material behavior of paper is not sufficient for numerical analysis, yet. Searching for material modells of paper, the two-dimensional nonlinear law by Paetow is to be mentioned [10]. This refers to the machine and the cross direction and describes the stress-strain behavior of paper over the entire area of deformability.

Concerning to the thickness direction the works of Pfeiffer [12] and van Haag [11] are to be mentioned, which deduce one-dimensional material laws for paper for typical pressure ranges in winding and calandering. The material law by van Haag was deduced following the compliance model by Paetow. Pfeiffer deduced a material law for the thickness direction, which is based on an exponential function. A three-dimensional material law for paper, that describes the real material behavior was not found.

In summary we can say, that the correlations of the shear-slitting process, as well as the influence of the material properties and other parameters on the slitting process cannot be clearly described today.

METHOD FOR THE THEORETICAL ANALYSIS OF THE SHEAR-SLITTING PROCESS

The emphasis of the theoretical analysis of the shear slitting process is the investigation of the kinetics and kinematics of the slitting process under variation of the influence parameters: the material behavior, the slitting procedure and the cutting tool.

In context of the material behavior it has to be clarified, which degree of idealization is acceptable for a adequate modelling of the slitting process. The idealization degree of the material behavior is increased gradually and adapted to the real material behavior of paper. In a first step a linear isotropic material behavior, in a second a linear orthotropic and in a third step a nonlinear othotropic material behavior is assumed (viz. Fig. 2). With these idealization levels the stress-strain states of the slitting process are determined. Since the slitting process is a high complex procedure this states can be determined only numerically. For the numerical simulation of the slitting process the finite-element-method (FEM) is used with a variation of the slitting procedure and the cutting tools.

These variations are done with the FEM-system Marc&Mentat. In the context of this publication first intermediate results from this research project are presented.

Development of a three-dimensional material law

A general, three-dimensional material law is shown in formula (1):

$$\begin{pmatrix}\sigma_{11}\\ \sigma_{22}\\ \sigma_{33}\\ \sigma_{44}\\ \sigma_{55}\\ \sigma_{66}\end{pmatrix} = \begin{pmatrix} C_{11} & C_{12} & C_{13} & C_{14} & C_{15} & C_{16}\\ C_{21} & C_{22} & C_{23} & C_{24} & C_{25} & C_{26}\\ C_{31} & C_{32} & C_{33} & C_{34} & C_{35} & C_{36}\\ C_{41} & C_{42} & C_{43} & C_{44} & C_{45} & C_{46}\\ C_{51} & C_{52} & C_{53} & C_{54} & C_{55} & C_{56}\\ C_{61} & C_{62} & C_{63} & C_{64} & C_{65} & C_{66}\end{pmatrix} \cdot \begin{pmatrix}\varepsilon_{11}\\ \varepsilon_{22}\\ \varepsilon_{33}\\ \varepsilon_{44}\\ \varepsilon_{55}\\ \varepsilon_{66}\end{pmatrix} \qquad (1)$$

This description covers the stress tensor σ, the strain tensor ε and the stiffness tensor $\mathbf{C}$.

The simplest idealization degree for the modelling of material behavior is the linear isotropic behavior. As a result of linear isotropic behavior the material properties are independent of orientation and there is a proportional correlation between applied stress and strain. The proportionality factor is called in the case of a normal strain Young's modulus E and in the case of a shear strain shear modulus G. A further material constant is known as Poisson's ratio μ, which is a measure for the deformation transverse to the load direction. The stiffness matrix for linear, three-dimensional isotropic materials can be described by use of this three material constants as follows:

$$C_{ij} = \begin{bmatrix} E\frac{1-\mu}{X} & E\frac{\mu}{X} & E\frac{\mu}{X} & 0 & 0 & 0\\ & \frac{1-\mu}{X} & E\frac{\mu}{X} & 0 & 0 & 0\\ & & \frac{1-\mu}{X} & 0 & 0 & 0\\ S & & & G & 0 & 0\\ & Y & & & G & 0\\ & & M & & & G\end{bmatrix} \qquad (2)$$

with $X = (1+\mu)\,(1-2\mu)$

The orthotropic material behavior is a closer-to-reality description of the material behavior. This behavior means, that the material possesses orientation dependent, orthogonal material properties. By experimental investigations of Paetow [10] it was proven that the material behavior of paper can be assumed as orthotropic concerning to MD and CD. Under the assumption that paper possesses extreme stiffness values

concerning to the thickness direction, we can indicate the stiffness matrix for linear, orthotropic materials:

$$C_{ij} = \begin{pmatrix} E_{11}\frac{1-\mu_{23}\mu_{32}}{X} & E_{11}\frac{\mu_{21}+\mu_{23}\mu_{31}}{X} & E_{11}\frac{\mu_{31}+\mu_{21}\mu_{32}}{X} & 0 & 0 & 0 \\ & E_{22}\frac{1-\mu_{13}\mu_{31}}{X} & E_{22}\frac{\mu_{32}+\mu_{12}\mu_{31}}{X} & 0 & 0 & 0 \\ & & E_{33}\frac{1-\mu_{12}\mu_{21}}{X} & 0 & 0 & 0 \\ S & & & G_{23} & 0 & 0 \\ & Y & & & G_{13} & 0 \\ & & M & & & G_{12} \end{pmatrix} \quad (3)$$

with

$$X = 1-\mu_{12}\mu_{21}-\mu_{13}\mu_{31}-\mu_{23}\mu_{32}-2\mu_{13}\mu_{21}\mu_{32}$$

Considering that paper exhibits a strongly nonlinear material behavior the formula (3) has to be extended. In the compliance law by Paetow the nonlinearity is described with use of a nonlinear, orientation dependent term. This term was extended for the thickness direction and coupled with the linear three-dimensional material law (3) for orthotropic materials. Thus the nonlinear three-dimensional material law for paper (4) is received:

$$\begin{pmatrix} \sigma_{11} \\ \sigma_{22} \\ \sigma_{33} \\ \sigma_{23} \\ \sigma_{13} \\ \sigma_{12} \end{pmatrix} = A \begin{pmatrix} \frac{E_{11}^{ini}(1-\mu_{23}\mu_{32})}{X} & \frac{E_{11}^{ini}(\mu_{21}+\mu_{23}\mu_{31})}{X} & \frac{E_{11}^{ini}(\mu_{31}+\mu_{21}\mu_{32})}{X} & 0 & 0 & 0 \\ & \frac{E_{22}^{ini}(1-\mu_{13}\mu_{31})}{X} & \frac{E_{22}^{ini}(\mu_{32}+\mu_{12}\mu_{31})}{X} & 0 & 0 & 0 \\ & & \frac{E_{33}^{ini}(1-\mu_{12}\mu_{21})}{X} & 0 & 0 & 0 \\ S & & & G_{23}^{ini} & 0 & 0 \\ & Y & & & G_{13}^{ini} & 0 \\ & & M & & & G_{12}^{ini} \end{pmatrix} \cdot \begin{pmatrix} \varepsilon_{11} \\ \varepsilon_{22} \\ \varepsilon_{33} \\ \varepsilon_{23} \\ \varepsilon_{13} \\ \varepsilon_{12} \end{pmatrix} \quad (4)$$

with

$$A = \frac{1}{1+\frac{\overline{E}_{11}^{ini}}{\overline{S}_{11}}\overline{\varepsilon}^{res}} \; ; \; X = 1-\mu_{12}\mu_{21}-\mu_{13}\mu_{31}-\mu_{23}\mu_{32}-2\,\mu_{13}\mu_{21}\,\mu_{32} \; ; \; \varepsilon^{res} = \sqrt{\frac{\varepsilon_I^2+\varepsilon_{II}^2+\varepsilon_{III}^2}{1+\mu_{12}^2+\mu_{13}^2+\mu_{23}^2}}$$

The non-linearity term A depends on the load size and the load direction. $\overline{\varepsilon}^{res}$ is a kind of total strain and is responsible for the load dependancy of A. E_{11}^{ini} – is an initial Young´s modulus and the $\overline{S}_{11}$ is the tension border defined by Paetow. Both terms are dependent on the load direction.

Material parameters for paper

For the application of the three-dimensional, linear orthotropic material law for paper 12 direction-bound material constants like: Young´s moduli E_{ii}, the Poisson´s ratios μ_{ij} and the shear moduli G_{ij} are necessary. For isotropic materials it can be shown that E, G and μ are coupled with one another. A comparable relation for orthotropic materials was not found. Due to the energy constrain Poisson´s ratios and Young´s moduli are connected as follows:

$$\frac{\mu_{12}}{E_{11}} = \frac{\mu_{21}}{E_{22}} \tag{5}$$

Anyway 9 independent material parameters still remain, which have to be determined experimentally. Due to the geometrical dimensions and the nonlinear material properties of paper the determination of these material parameters is difficult.

Detailed numerical data of this material constants are not completely present until today. In [10] numerical data for the material parameters in MD and CD are found. Concerning the thickness direction characteristic values for individual types of paper are found in [11] and [14]. Be aware, that the experimental loads used for determing these material constants were much lower than the expected loads in the slitting process. However they make a simulation possible and allow a reduced interpretation of the results. For the following simulations the Young´s moduli of the MD, CD and thickness direction (E_{11}, E_{22} and E_{33}), the three shear moduli (G_{12}, G_{23} and G_{31}) and the three Poisson´s ratios (μ_{12}, μ_{23} and μ_{31}) are needed.

The material constants, which were selected for the following simulation, are to be found in table 1. The dependence of the selected Young´s moduli from the strain level is shown in figure 3, where the initial sizes are marked. For the linear orthotropic behavior a representative constant value for the Young´s modulus has to be selected from these courses. Since the main load during the slitting process runs in thickness direction and lateral contractions in MD and CD are small, only small tensions in MD and CD are expected. Therefore the initial Young´s moduli are used for these directions. Because the FEM–calculation have to simulate the entire compression phase up to the slitting phase, a Young modulus of 130 N/mm^2 is selected for the thickness direction instead of the initial Young´s modulus. This size corresponds to a deformation of the paper web in thickness direction of 40 %.

In order to be able to compare the isotropic calculation with the orthotropic calculation, the isotropic Young´s modulus was selected so, that in case of same penetration depth of the cutting tool the introduced cutting force is equal to the orthotropic case. This demand leads to an isotropic Young´s modulus of 170 N/mm^2. In figure 4 all selected Young´s moduli are summarized. The Poisson´s ratios and the shear moduli were estimated or selected following [10].

FEM - Modelling of the geometric and boundary conditions

The dimensions of the reference model are shown in figure 5. The length of the paper web model is 500 µm in MD, the thickness is 100 µm. These dimensions ensure that the whole slitting area can be observed. The FE-model is two-dimensional and a state of plane strain is assumed. Due to the symmetrical structure of the geometry and the symmetrical load, the point in the center of the paper web will have no displacement and is therefore fixed. The cutting tools are modelled as rigid bodies and their movement direction is only perpendicular to the paper web. The displacements of the cutting tools are given as boundary conditions. The displacements are applied gradually up to a maximum total material compression of 20 %. The cutting tools touch down in the first load step on the paper web and penetrate into the paper with increments of 0,5 µm. The radius used for the knife point is 5 µm, because this size is regarded as sharp [15].

For the FE - modelling (fig 6) square 4-nodes-elements without subnodes are used. These elements are suitable for the modelling of the existing state of plane strain and for the modelling of contact between the different materials paper and steel. Furthermore direction-bound material properties can be given for these elements, so that orthotropic material behavior can be modelled. In order to make a local and global view of the arising tension and distortion fields possible, different meshing densities were selected. Because the shear slitting process causes high gradients in stress and strain within the area of the slitting line, a large dissolution of the mesh is necessary in this range. Wide distant ranges get along with a rough mesh, because here are only small gradients expected. An advantage of this purposeful meshing density is on the one hand the increased computational accuracy and on the other hand a smaller computing time.

The material behavior is modelled as linear isotropic and additionally as linear orthotropic. A nonlinear orthotropic material behavior has to be done in future work. In the following the states of stress and strain for the reference nodes A, B and C (see fig. 6 and 7) are analyzed in particular.

FEM – Simulation: Reference model

In figure 8 the normal stresses in MD and ZD at the paper surface are represented for linear isotropic and linear orthotropic material behavior at the time of maximum depth of the cutting tool. The course of the compression in ZD is similar for both cases. The compressive stress is locally limited in the contact zone. The maximum in compressive stress is slightly higher in the isotropic model, due to the slightly higher Young´s modulus in ZD. The stress course in MD shows a strong dependence on the used material law. In the isotropic case there is a tension zone directly underneath the knife point (reference node A) whereby the wedge surface of the cutting tool (reference node B) shows compressive stresses. Outside the contact zone small tensions are recognizable as reaction to the penetration of the cutting tool into the paper.

In the orthotropic case these tensions develop more clearly, due to the substantially higher Young´s modulus in MD. The stress course in MD of the whole contact zone is compressive, but in the area of the knife point reduced stresses can be found. However, no tension zone exists, as can be seen in the isotropic case.

The course of the normal stresses in MD and ZD along the paper thickness are represented in figure 9. It is recognizable that the high stress field in the isotropic, as well as in the orthotropic case, is limited to an area close to the contact zone. The already mentioned dependence of the tension in MD by the material behavior is found again in this illustration. At the sheet center (reference node C) moderate compressive stresses in ZD and small tensions in MD are formed in both cases. Whereby the tensile stresses in MD are significantly higher in the orthotropic case compared to the isotropic case.

In figure 10 the states of stress and strain at the reference node A are shown in dependence of the penetration depth of the cutting tool. The depth is expressed by the average total compression of the sheet (0-20%). In the isotropic case the states of stress and strain for ZD and MD are forming a straight line, whose gradient corresponds to the isotropic Young´s modulus. When the cutting tool starts to penetrate the paper, compressive stresses are formed in ZD as well as in MD. While the compressive stresses grow with increasing penetration in ZD, the stresses in MD reach a maximum pressure at the point of 5-10% average total compression of the sheet. Further penetration of the cutting tool yields to a decrease of compressive stress and ends up in tensile stresses.

In the orthotropic case the states of stress and strain are on two straight lines, whose gradients correspond to the orthotropic Young´s moduli E_{11} and E_{33}. Again the compressive stresses in ZD increase with progressing penetration of the cutting tool, whereby the stresses in MD reach a maximum compressive stress and start to decrease further on.

This behavior can be explained as follows. At the beginning of the compression procedure compressive stresses are formed in all directions, in accordance with the theory of Hertz. The reduction of the compressive stresses in MD with progressing compression can be explained by the material displacement, due to the increasing wedge effect of the penetrating cutting tools.

Studying the failure mechanism of the paper, it is very usefull to represent the stress states of places exposed to maximum stresses by use of Mohr´s circle. Figure 11 shows Mohr´s circles for the reference nodes A and C. The stress differences in MD comparing isotropic or orthotropic modelling causes a shift of Mohr´s circle toward tension, whereas the diameter and thus the maximum arising shear stress remains almost unchanged. In both cases the shear-yield-border is clearly exceeded. If one compares Mohr´s circles at the surface (reference node A) and in the sheet center (reference node C), the locally limited effect of the force application is clearly seen. In the sheet center no failure mechanism is exceeded so far.

FEM – Simulation: Variation of the geometry of the cutting tools

In practice the geometry of the cutting tools mainly differs by the wedge angle and the knife point radius, which continues to increase with increasing wear. In order to examine the influence of the geometry on the stress distribution within the sheet, a near model was set up with an increased wedge angle from 22° to 55° (model 3), as well as a model with an increased point radius from 5 to 10 µm(model 4, table 2). Both models calculations were performed by applying the same outer force as in the reference model

(model 2). Drawing Mohr´s circle at the reference node A and comparing the stress states of these models with the reference model, only negligibly small differences are represented in accordance with fig. 12.

CONCLUSION

The knowledge of the kinetic and kinematic connections of the shear slitting process are necessary for the increase of the productivity, the cut quality and the blade durability. It was shown that with the finite-element-method a numeric computing procedure is available, which can compute the complex, three-dimensional states of stress and strain during the slitting procedure. The quality of the obtained results depends highly, on the used idealization degree of the material law. The interpretation of the results permits a description of the slitting process on the basis of states of stress and strain and a discussion of the failure mechanism by use of Mohr´s circle. A better knowledge of the material behavior of paper can obtain an increase of the model accuracy in future. Additionally the failure mechanism of paper can be better described, as well as the separation of the individual slitting phases. The implementation of any failure mechanism of paper in the FE-model will enable, beside the compression phase, the numerical analysis of the slitting - and tearing phase as well.

REFERENCES

1 E.G. Welp, „Forschungsinitiative Papierausrüstung", Das Papier, Vol. 49, No. 10A, 1995, pp. V139-V148.

2 Th. Hülsmann, „Messerverschleiß in Querschneideinrichtungen von Verpackungsmaschinen", Verpackungsrundschau, Vol. 34, No. 12, 1983, pp. 87-93.

3 M. Feiler, „Ein Beitrag zur Klärung der Vorgänge beim Schneiden dünner flächiger Materialien", PhD. Thesis, 1970.

4 T. Hombach, H. Sturm, „Probleme und Erkenntnisse beim Schneiden bahnförmiger Materialien", Das Papier, Vol. 29, 1975, pp. 385-392.

5 C. Stromberger, Th. Thomsen, „Glatte Lochwände beim Lochen", Werkstatt und Betrieb, Vol.10, 1965, pp. 739-747.

6 O. Kienzle, „Der Vorgang des Schneidens", Mikrotechnik, Vol. X, 1956, Nr. 6.

7 G. Timmerbeil, „Untersuchungen des Schneidvorgangs bei Blech, insbesondere beim geschlossenen Schnitt", PhD. Thesis, TH Hannover, 1956.

8 E. Siebel, „Werkstoffmechanik", VDI - Zeitschrift, 1953, pp. 27- 33.

9 K. Weyl, „Schnittkräfte an Papierschneidemaschinen", Allg. Anz. für Buchbindereien, Hefte 2, 3, 4, 5, 1962.

10 R. Paetow, „Über das Spannungs-Verformungs-Verhalten von Papier", PhD. Thesis, TH Darmstadt, 1991.

11 Rolf van Haag, „Über die Druckspannungsverteilung und die Papierkompression im Walzenspalt eines Kalanders", PhD. Thesis, TH Darmstadt, 1993.
12 J. D. Pfeiffer, „Principles of Web Slitting" , Proceedings of the Fourth International Conference on Web Handling, Web Handling Centre, Stillwater, Oklahoma, June 1-4, 1997.
14 H. J. Schaffrath, „Über das Kompressions- und Reibverhalten von Papier vor dem Hintergrund des Rollenwickelns", PhD. Thesis, TH Darmstadt, 1993.
15 H. Hofer, „Stanzen von Karton und Wellpappe in Theorie und Praxis" , Papier und Kunststoffverarbeiter, Vol. 2, 1997, pp. 28 -33.

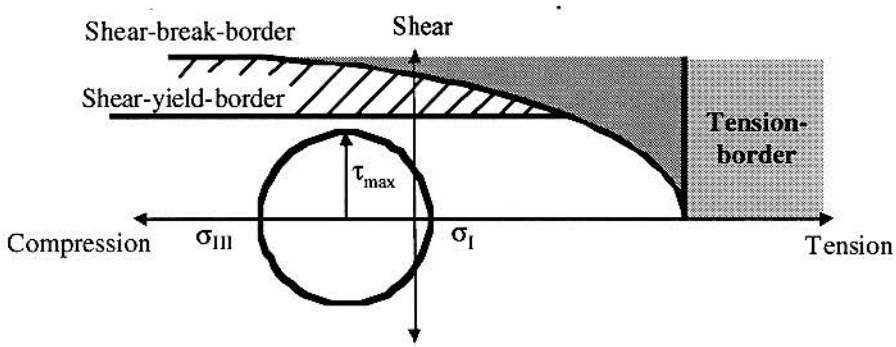

Fig. 1 Failure hypothesis

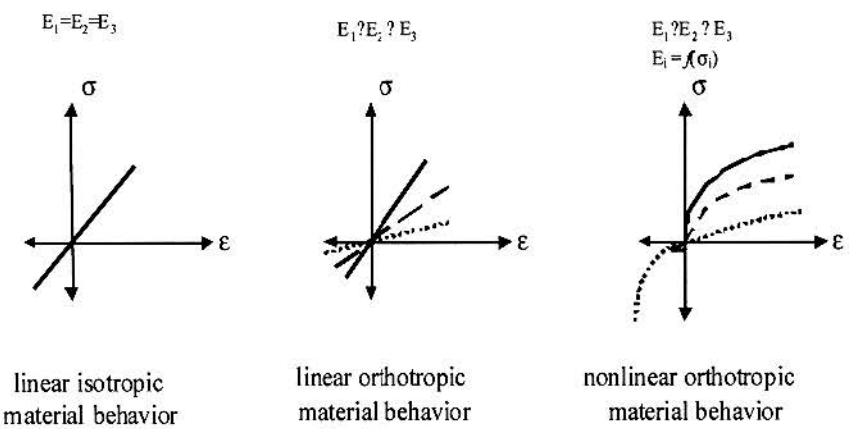

Fig. 2 Degrees of idealisation of the material behavior

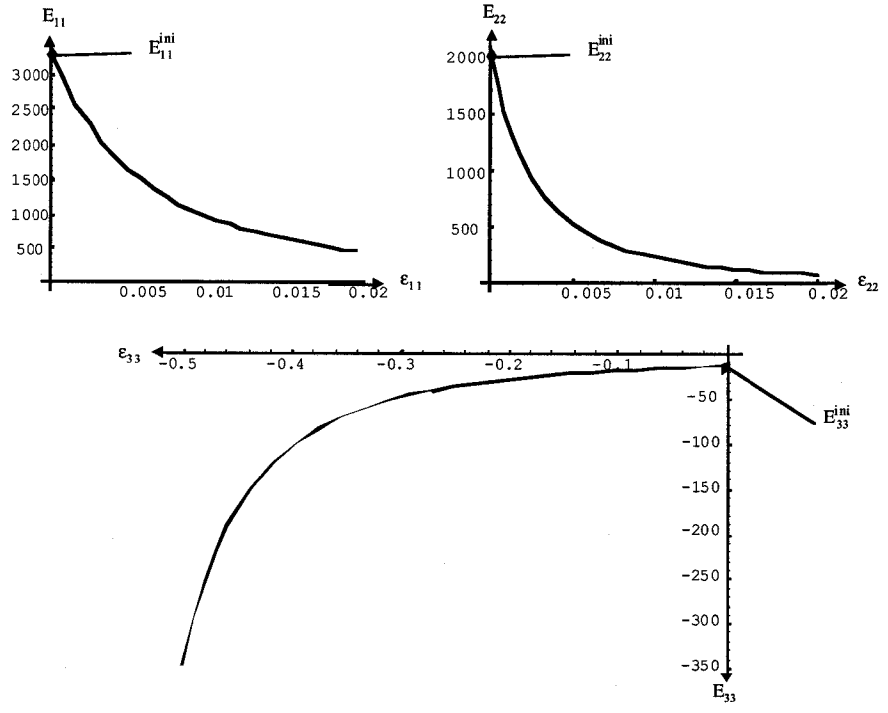

Fig. 3 Orientation- and load dependent Young´s modulus

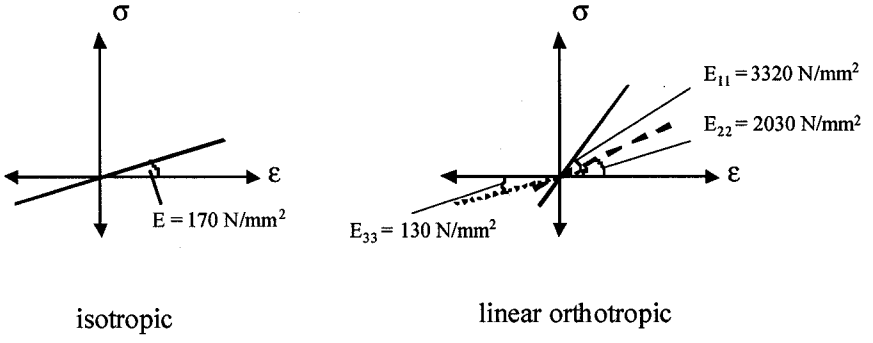

Fig. 4 Isotropic and orthotropic modelling of the material behavior

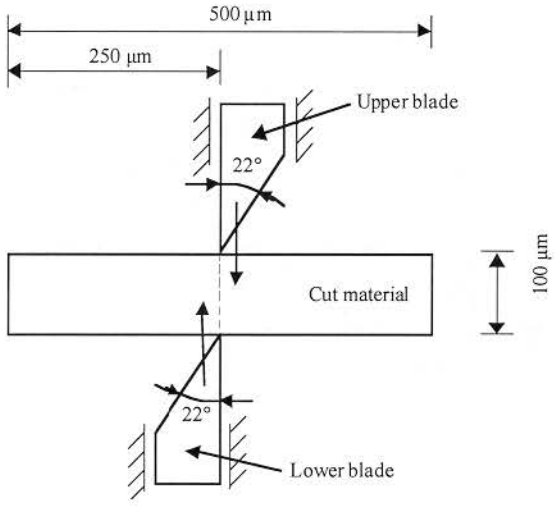

Fig. 5 Geometry of the reference model

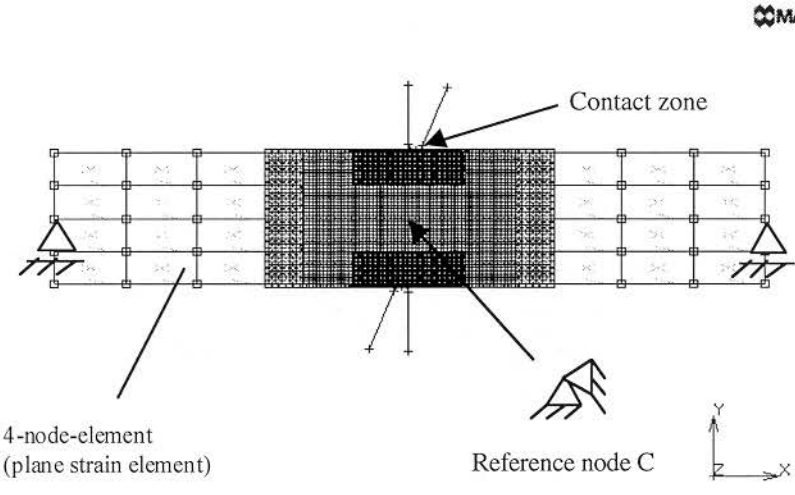

Fig. 6 FE-Reference model

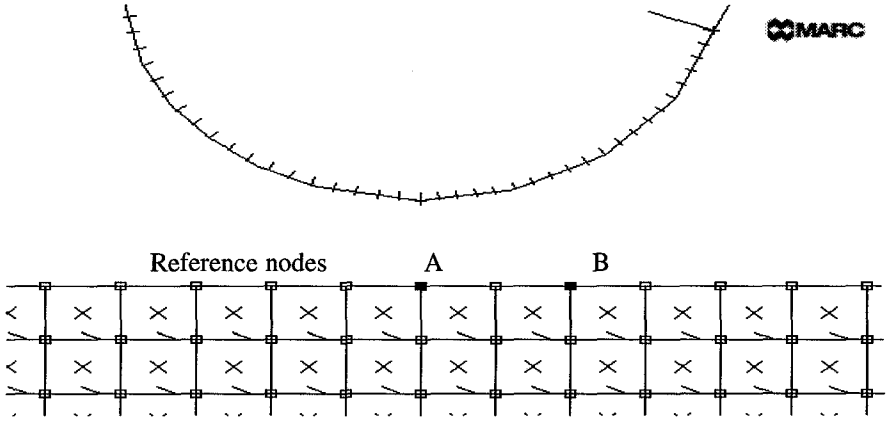

Fig. 7 Contact zone of the reference model

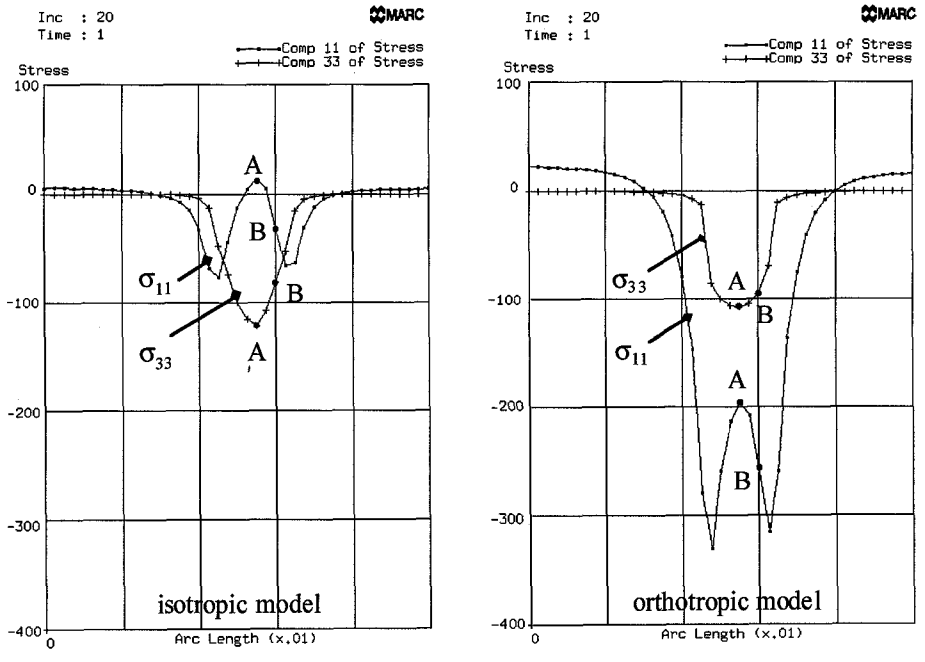

Fig. 8 Normal stresses σ_{11} (MD) and σ_{33} (ZD) at the paper surface for isotropic and orthotropic material behavior

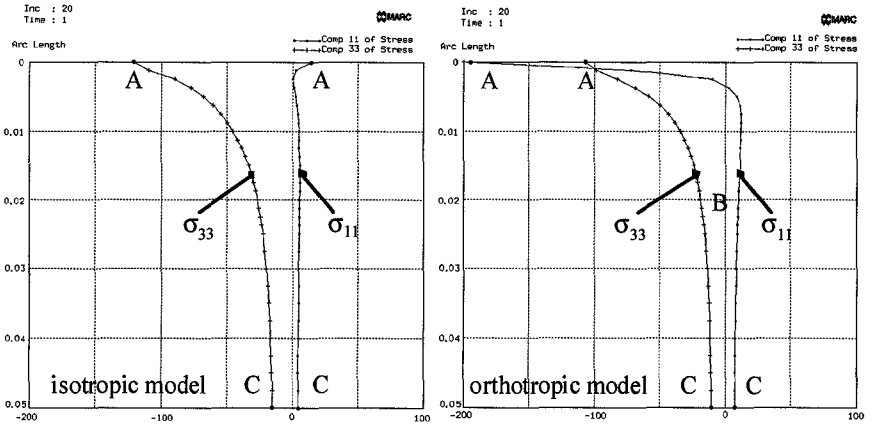

Fig. 9 Normal stresses σ_{11} (MD) and σ_{33} (ZD) along the paper thickness for isotropic and orthotropic material behavior

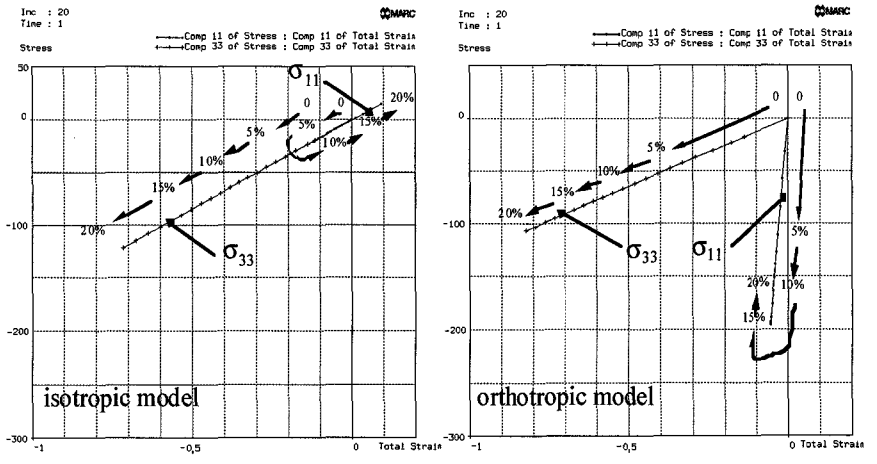

Fig. 10 States of stress and strain of the reference node A as a function of total compression of the paper

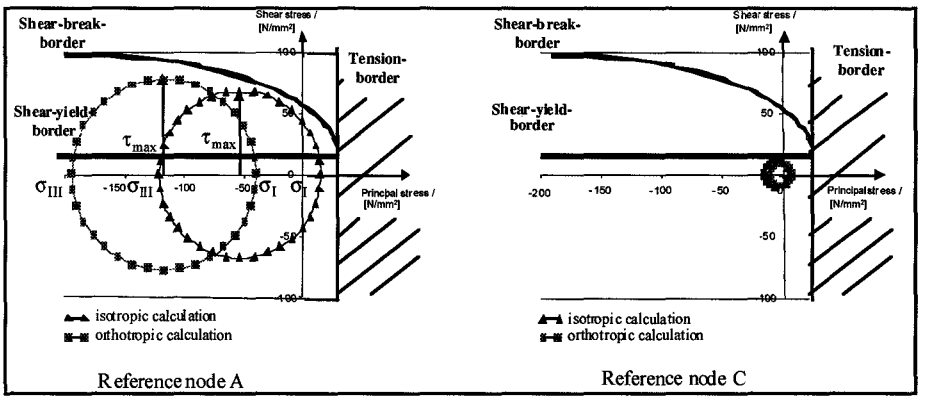

Fig. 11 Mohr´s circle for the reference nodes A and C

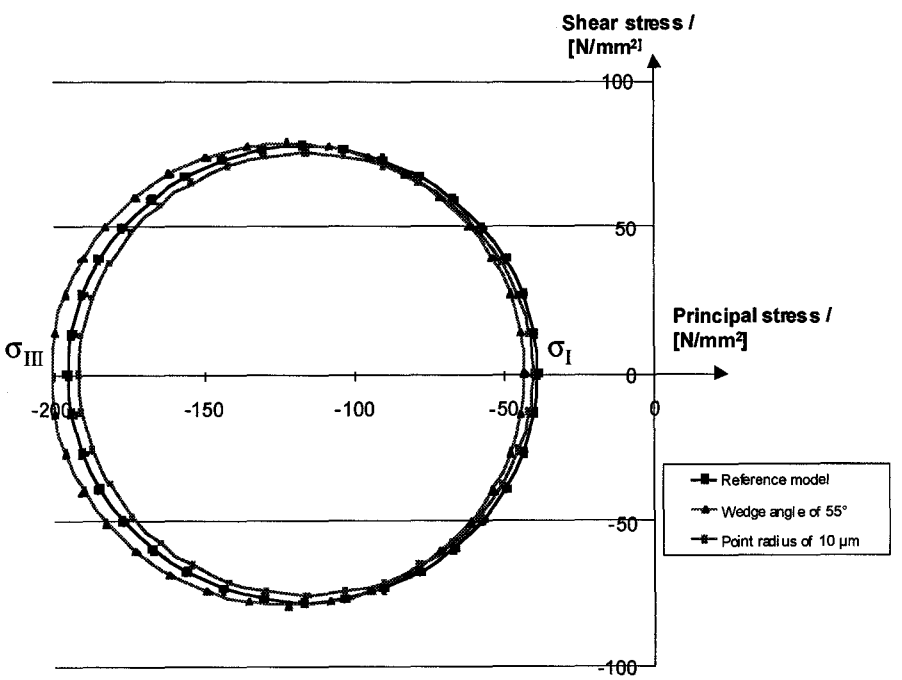

Fig. 12 Mohr´s circle for the reference nodes A

	isotropic calculation	orthotropic calculation
Young´s modulus, E_{11}	170 N/mm^2	3320 N/mm^2
Young´s modulus, E_{22}		2030 N/mm^2
Young´s modulus, E_{33}		130 N/mm^2
Shear modulus, G_{12}	84,16 N/mm^2	1034 N/mm^2
Shear modulus, G_{23}		100 N/mm^2
Shear modulus, G_{31}		80 N/mm^2
Poisson´s ratio, μ_{12}	0,01	0.2
Poisson´s ratio, μ_{23}		0.0002
Poisson´s ratio, μ_{31}		0.01

Table 1 Material constants for the FEM - calculation

	Reference model	Model 2	Model 3	Model 4
Material behavior	isotropic	orthotropic	orthotropic	orthotropic
Wedge angle	22°	22°	55°	22°
Knife point radius	5 µm	5 µm	5 µm	10 µm

Table 2 Material constants for the FEM - calculation

E.G. Welp and E. Wolf
Theoretical Analysis of Shear Slitting of Paper on the Basis of a Three-Dimensional Material Law
6/8/99 Session 2 9:25 - 9:50 a.m.

Question - Nanda Vaidyanathan, Prestech
My question is on the Finite Element Mesh. At the point of contact of your blade of the web, you have a very fine mesh and as you go further to the left and the right the mesh is getting coarse. But when I saw the picture a little more clearly you don't gradually increase the meshes and merge and you have a lot a discontinuity from the area of very fine mesh to the area of very coarse mesh and that will cause a discontinuity in your solution. How did you account for that?

Answer – E. Wolf, Ruhr University
There is a refinement-function implemented in the used finite-element-system. This was applied in the area of the slitting line. This application was also done in a distance of the slitting line, too, but it had no influence on the achieved results.